The North Atlantic Thermohaline Circulation Simulated by the GISS Climate Model during 1970-99

Larissa Nazarenko[1,*], Nickolai Tausnev[2] and James Hansen[3]

[1]*Columbia University/NASA Goddard Institute for Space Studies, New York, NY, USA*
[2]*SSP LLC/NASA Goddard Institute for Space Studies, New York, NY, USA*
[3]*NASA Goddard Institute for Space Studies, New York, NY, USA*

[Original manuscript received 12 April 2006; in revised form 3 January 2007]

ABSTRACT *Evidence based on numerical simulations is presented for a strong correlation between the North Atlantic Oscillation (NAO) and the North Atlantic overturning circulation. Using an ensemble of numerical experiments with a coupled ocean-atmosphere model including both natural and anthropogenic forcings, it is shown that the weakening of the thermohaline circulation (THC) could be delayed in response to a sustained upward trend in the NAO, which was observed over the last three decades of the twentieth century, 1970–99. Overall warming and enhanced horizontal transports of heat from the tropics to the subpolar North Atlantic overwhelm the NAO-induced cooling of the upper ocean layers due to enhanced fluxes of latent and sensible heat, so that the net effect of warmed surface ocean temperatures acts to increase the vertical stability of the ocean column. However, the strong westerly winds cause increased evaporation from the ocean surface, which leads to a reduced fresh water flux over the western part of the North Atlantic. Horizontal poleward transport of salinity anomalies from the tropical Atlantic is the major contributor to the increasing salinities in the sinking regions of the North Atlantic. The effect of positive salinity anomalies on surface ocean density overrides the opposing effect of enhanced warming of the ocean surface, which causes an increase in surface density in the Labrador Sea and in the ocean area south of Greenland. The increased density of the upper ocean layer leads to deeper convection in the Labrador Sea and in the western North Atlantic. With a lag of four years, the meridional overturning circulation of the North Atlantic shows strengthening as it adjusts to positive density anomalies and enhanced vertical mixing. During the positive NAO trend, the salinity-driven density instability in the upper ocean, due to both increased northward ocean transports of salinity and decreased atmospheric freshwater fluxes, results in a strengthening overturning circulation in the North Atlantic when the surface atmospheric temperature increases by 0.3°C and the ocean surface temperature warms by 0.5° to 1°C.*

RÉSUMÉ *[Traduit par la rédaction] Nous présentons des preuves basées sur des simulations numériques d'une forte corrélation entre l'oscillation nord-atlantique (ONA) et la circulation de renversement dans l'Atlantique Nord. Au moyen d'un ensemble d'expériences numériques avec un modèle couplé océan-atmosphère qui inclut à la fois les forçages naturel et anthropique, nous montrons que l'affaiblissement de la circulation thermohaline pourrait être retardé par suite d'une tendance à la hausse soutenue dans l'ONA, tendance qui a été observée au cours des trois dernières décennies du vingtième siècle, soit la période 1970–1999. Le réchauffement général et l'augmentation des transports horizontaux de chaleur des tropiques vers l'Atlantique Nord subpolaire font plus que compenser le refroidissement causé par l'ONA des couches supérieures de l'océan à cause de l'augmentation des flux de chaleur latente et sensible, de sorte que l'effet net des températures plus élevées de la surface de l'océan fait augmenter la stabilité verticale de la colonne océanique. Cependant, les forts vents d'ouest entraînent une évaporation accrue à la surface de l'océan, ce qui mène à un flux d'eau douce réduit dans la partie ouest de l'Atlantique Nord. Le transport horizontal vers le pôle des anomalies de salinité à partir de l'Atlantique tropical est le principal contributeur de l'accroissement de salinité dans les régions de plongée d'eau de l'Atlantique Nord. L'effet des anomalies positives de salinité sur la densité de la surface océanique annule l'effet opposé du réchauffement accru de la surface océanique, ce qui entraîne un accroissement de la densité à la surface dans la mer du Labrador et dans la région de l'océan au sud du Groenland. La densité accrue des couches supérieures de l'océan occasionne une convection plus profonde dans la mer du Labrador et dans l'ouest de l'Atlantique Nord. Avec un retard de quatre ans, la circulation de renversement méridienne dans l'Atlantique Nord se renforce en réponse aux anomalies de densité positives et au mélange vertical accru. Durant la tendance positive de l'ONA, l'instabilité de densité (liée à la salinité) dans la couche supérieure de l'océan, qui résulte à la fois de l'augmentation des transports océaniques de salinité vers le nord et de la diminution des flux d'eau douce atmosphériques, entraîne un renforcement de la circulation de retournement dans l'Atlantique Nord quand la température atmosphérique à la surface augmente de 0,3 ºC et que la température de surface de l'océan s'élève de 0,5 à 1,0 ºC.*

*Corresponding author's e-mail: lnazarenko@giss.nasa.gov

1 Introduction

A significant fraction of climate variability in the North Atlantic is strongly influenced by fluctuations in the strength of the Icelandic low and the Azores high atmospheric pressure centres, which are referred to as the North Atlantic Oscillation (NAO) (Hurrell, 1995; Hurrell and van Loon, 1997; Thompson et al., 2000). The NAO, derived from observational records, has shown a trend towards the positive phase of the oscillation since the early 1970s with warmer northern hemisphere land temperatures (Hurrell, 1996). The positive phase of the NAO reflects enhanced mid-latitude westerlies, which in turn influence the intensities of atmosphere-ocean exchanges of heat, fresh water and momentum (Cayan, 1992a, 1992b; Hurrell, 1996; Visbeck et al., 1998). Since the ocean circulation is wind and buoyancy driven, the atmospheric circulation, the NAO in particular, may influence the vertical density structure of the ocean water column, which in turn leads to an alteration of the ocean thermohaline circulation (Timmermann et al., 1998; Delworth and Dixon, 2000; Latif et al., 2000).

Although some studies (Shindell et al., 1999; Fyfe et al., 1999; Hu and Wu, 2004) assert that the upward trend of the NAO is a result of increasing greenhouse gases, other research shows that the trend in the NAO can be explained by a combination of internal variability and greenhouse forcing (Osborn et al., 1999; Osborn, 2004). Osborn (2004) shows that other external climate forcings may have contributed to the observed NAO variability. Furthermore, it is important to assess the effect of the NAO trend on other components of the climate system, in particular on the North Atlantic thermohaline circulation (THC). Although most of the coupled climate models predict a weakened THC with warming conditions (Manabe and Stouffer, 1999; Rahmstorf and Ganopolski, 1999; Russell and Rind, 1999; Wood et al., 1999; Hu et al., 2004), there are some coupled models that show little response of the Atlantic THC to increased CO_2 (Latif et al., 2000; Gent, 2001; Sun and Bleck, 2001). The ocean surface warming is responsible for most of the THC weakening, and the enhanced poleward transport of moisture, reflected in increased precipitation and river run-off, also contribute to stabilizing the ocean stratification and reducing the formation of North Atlantic Deep Water (NADW).

The enhanced winds during the positive NAO phase cause heat loss from the ocean surface, which leads to cooling and increases the density of the upper ocean. This strong cooling in the North Atlantic surface ocean tends to cancel out at least part of the effect of the reduced surface densities from previously described warming. It has been noted in earlier studies that, on interannual timescales, surface ocean temperature and salinity anomalies develop directly in response to NAO air-sea heat and moisture flux anomalies (Bjerknes, 1964; Cayan, 1992a, 1992b; Deser and Blackmon, 1993; Kushnir, 1994; Walter and Graf, 2002). On longer timescales of several decades, surface ocean temperature and salinity anomalies are primarily driven by changes in meridional ocean transports of heat and salt (Halliwell, 1998; Wu and Gordon, 2002).

The intensified air-sea moisture exchanges in the North Atlantic cause an enhancement of both precipitation and evaporation, associated with an overall increase in greenhouse gas warming during the last few decades of the twentieth century and strengthening of the westerly winds over the subpolar North Atlantic during the upward NAO trend. While freshening from increased precipitation and river run-off reduces the surface salinity, intensified evaporation causes an increase in salinity. These two opposing effects on salinity can lead to either stable vertical stratification of the ocean column or unstable vertical stratification and an increase in vertical mixing and convection. In addition to this, horizontal poleward transports of salinity are a contributing factor in compensating for the reduced salinity due to increased precipitation and river run-off. Some climate models (Timmermann et al., 1998; Latif et al., 2000) predict a stable North Atlantic THC due to the increasing salinities of the ocean masses flowing from the tropics toward the regions of strong mixing and convection.

This paper examines the effect of the upward trend in the NAO on the North Atlantic climate and, in particular, on the North Atlantic THC during the last three decades of the twentieth century, 1970–99. We explore opposing effects on the surface ocean density and the stability of the ocean column in the North Atlantic. Our attention will be focused on the physical mechanisms that lead to an increase in mixing and convection in the sinking regions of the North Atlantic and also influence the stability of the meridional overturning circulation.

2 Model description

We use the National Aeronautics and Space Administration (NASA) Goddard Institute for Space Studies (GISS) General Circulation Model (GCM) version III (Schmidt et al., 2006) with 4 by 5 degree horizontal resolution and 20 vertical layers, with the model top at 0.1 hPa. The basic physics of the model is similar to that used in the climate studies of Hansen et al. (2002) but includes some improvements as reported in Schmidt et al. (2006). The ocean model is a dynamic ocean model with the same horizontal resolution, and it has 13 vertical levels with the finer resolution at the top 100 m. The ocean model includes the K-profile parametrization (KPP) for vertical mixing (Large et al., 1994) and the Gent-McWilliams parametrization for mixing associated with mesoscale eddies (Gent and McWilliams, 1990). The sea-ice model includes both the dynamics and thermodynamics of ice cover in the Arctic and Southern oceans. The application of the same horizontal resolution for the ocean model as for the atmospheric model makes the coupled climate model very efficient for long experiments with different forcings.

The atmospheric and oceanic models are coupled by the fluxes of heat, fresh water and wind stress. These fluxes, calculated in the atmospheric model, are applied as forcings to the ocean model. The sea surface temperature (SST) and sea-ice cover are used as the lower boundary conditions for the atmospheric model. For ice-covered ocean grid points, the surface temperature of the sea ice is calculated in the atmospheric model from the balance of the longwave and shortwave radiation fluxes, sensible and latent heat fluxes and the conductive heat flux through the sea ice. We employ no flux correction in the heat, freshwater and momentum exchanges between the atmosphere and ocean to simulate a realistic climate.

The control experiment for the 1880 atmospheric composition has a drift of 0.06ºC per century and indicates a global

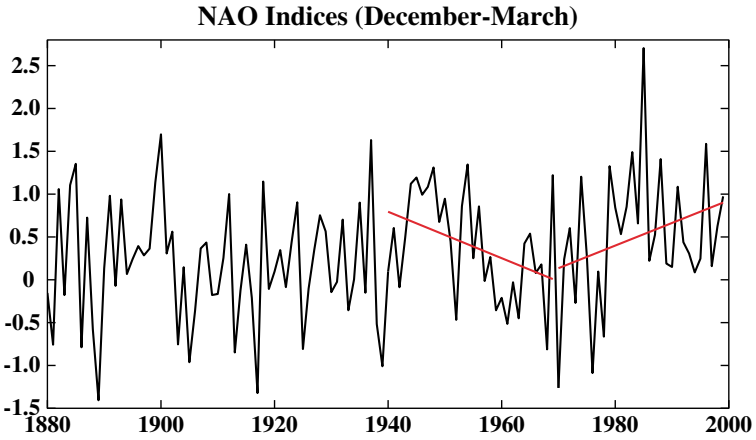

Fig. 1 Unsmoothed simulated ensemble-mean DJFM seasonally averaged NAO indices from the 5-run mean SLP anomalies. The pressure anomalies for each ensemble run are calculated as the pressure deviation from the respective DJFM mean pressures of the control experiment. The pressure anomalies are normalized by division of each run DJFM mean pressure by the long-term standard deviation of the control experiment. Linear trends for 1940–69 and 1970–99 are indicated by red lines.

mean surface air temperature of about 14ºC at modelled year 1000. The model climate sensitivity for doubled CO_2 is approximately 2.7ºC, which is within the range 3°±1ºC for doubled CO_2 inferred from paleoclimate evidence (Hansen et al., 1984, 1993). An ensemble of five simulations driven by increasing well-mixed greenhouse gases, solar irradiance, stratospheric water vapour derived from methane oxidation, tropospheric and stratospheric ozone, volcanic aerosols, changes in land use, and snow/ice albedo change proportional to the local soot deposition (Hansen et al., 2005) was performed beginning in 1880 and continuing until the end of 2002. Also included are tropospheric aerosols (sulphates, organic carbon and black carbon, sea-salt, dust and nitrates) and parametrized forms of the indirect effects of aerosols on clouds as described in Hansen et al. (2005). All runs of this ensemble used initial conditions at intervals of 25 years of the control experiment. This takes into account the unforced variability of the model. The control run is integrated with constant forcing corresponding to the year 1880. Here we focus on the time period 1970–99, when the NAO index exhibits the upward trend.

3 Results

a *Sea Level Pressure and the NAO Index*

Monthly mean sea level pressure (SLP) fields, averaged from December to March (DJFM), were taken from the averaged data of the 5-run ensemble. For our analysis, the NAO index is defined as the difference between the normalized DJFM-mean SLP anomalies at two stations near the subtropical high and the Icelandic low, respectively. The pressure anomalies for each ensemble run are calculated as the pressure deviation from the respective DJFM mean pressure of the control experiment. The pressure anomalies are normalized by division of each run DJFM mean pressure by the long-term standard deviation of the control experiment. The DJFM means of SLP are used for the NAO index calculations because, following Hurrell (1995) and Hurrell and van Loon (1997), the polarity and strength of the NAO are most pronounced during this season.

It has been noted from SLP observations since the beginning of the nineteenth century that the variability of the NAO index has not been uniform (Jones et al., 1997; Walter and Graff, 2002; Ostermeier and Wallace, 2003). Figure 1 shows the unsmoothed time series of the NAO indices from the 5-run mean SLP anomalies, which exhibits a negative trend in the NAO index from the 1940s to the 1960s and a positive trend in the NAO index over the last three decades of the twentieth century. Our experiments with natural and anthropogenic forcing show that the NAO index is characterized by more positive values since the early 1970s and shows higher year-to-year variability compared to the previous 30-year period (Fig. 1).

Our model reproduces a pronounced reduction in pressure over high polar latitudes for the last three decades, which was first noted in the Arctic SLP data from the Arctic Ocean Buoy Program and has been observed every year since 1988 (Walsh et al., 1996). In the middle latitudes the modelled SLP increases, contributing to the strengthened meridional pressure gradient and increased NAO index. The simulated SLP for the period 1970–99 is positively correlated with the NAO index over the middle latitudes of the North Atlantic and negatively correlated with the index over the Icelandic low and polar latitudes. This correlation pattern has been considered typical for a positive NAO phase since the 1970s (Hurrell, 1995; Thompson and Wallace, 1998; Thompson and Wallace, 2001).

b *Surface Air Temperature and Atmospheric Circulation*

The experiments with natural and anthropogenic forcings show that the surface air temperature (SAT) trends for 1970–99 are dominated by warming with the strongest area occurring over high latitudes. Under warming conditions, the large-scale pattern of SAT variability is similar to that accompanying the NAO; DJFM SAT is positively correlated with the NAO index over most of Europe and Scandinavia, the south-east United States, the subtropical Atlantic and the central Arctic while the surface temperature is negatively correlated over Greenland, the Labrador Sea and northern Africa

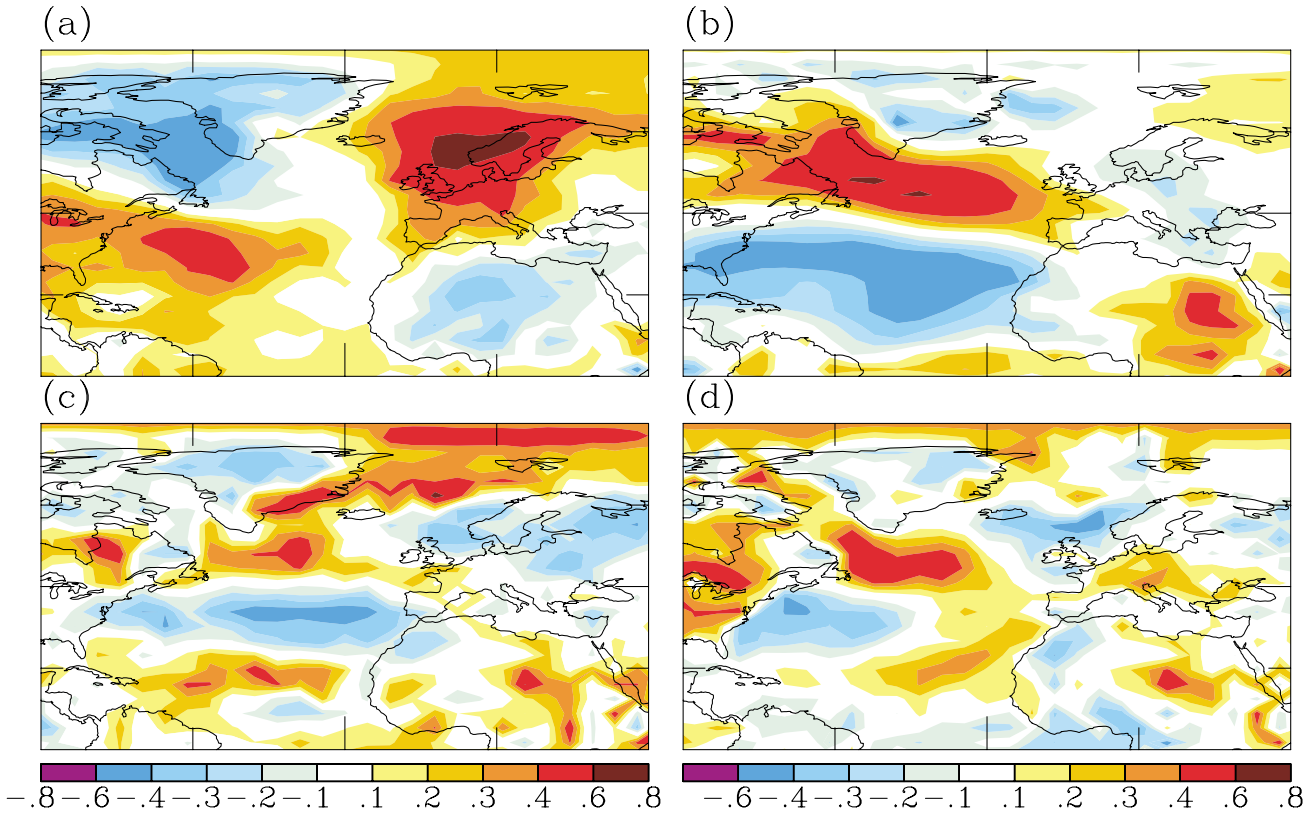

Fig. 2 Correlation map between the simulated ensemble-mean DJFM NAO index and (a) the simulated ensemble-mean DJFM surface air temperature; (b) the simulated ensemble-mean DJFM zonal component of surface wind; (c) the simulated ensemble-mean DJFM precipitation; and (d) the simulated ensemble-mean DJFM evaporation for the period 1970–99.

(Fig. 2a). These SAT and NAO correlations are consistent with advection by the large-scale atmospheric flow confirmed by observational data (van Loon and Rogers, 1978; Rogers and van Loon, 1979; Thompson et al., 2000).

The simulated surface wind trends for the 1970–99 winter season indicate an intensification of warm westerly flow across the Atlantic into Europe, a cold north-westerly flow from the central Arctic Ocean over the Labrador Sea, and a cold north-easterly flow over the Mediterranean region. This circulation pattern during the strong Icelandic low phase is reflected in the correlation between the NAO index and the zonal component of the surface wind (Fig. 2b); the zonal wind has a strong positive correlation with the NAO index to the south of the low pressure centre across the North Atlantic between 45°N and 65°N and has a negative correlation in the lower mid-latitudes between 20°N and 40°N (Fig. 2b).

The simulated NAO-related enhanced westerly flow across the North Atlantic brings warm, moist air over the northern part of Russia and Scandinavia, which results in increased precipitation over those areas. At the same time, drier-than-normal conditions are reproduced over southern Europe, the Mediterranean and the Middle East. The strengthened north-westerly winds lead to increased evaporation over the Labrador Sea and over the area south of Greenland, so that the modelled precipitation minus evaporation (P - E) shows enhanced evaporation over the Labrador Sea as well as over the western and subtropical Atlantic during high NAO index years. At the same time, the enhanced moisture convergence was reproduced from Iceland to Scandinavia. These moisture transport conditions are clearly simulated during the winter season but they can also be seen in the annual mean (P – E) (not shown).

The correlation between precipitation and the NAO index is positive over high polar latitudes including the northern part of Scandinavia as well as over the area of the Icelandic low, which corresponds to the increased moisture convergence during high NAO index years (Fig. 2c). The areas of negative correlation between precipitation and NAO index include central and southern Europe and the subtropical Atlantic with the strongest correlations reaching -0.6 over the subtropical high pressure centre. The model reproduces the NAO and precipitation correlation pattern quite well and is consistent with observational evidence (Hurrell and van Loon, 1997; Hurrell, 1995, 1996). From our model output, the positive correlation between evaporation and the NAO index (Fig. 2d) over the Labrador Sea and over the area south of Greenland coincides with the same area of positive correlation between the NAO index and the surface zonal wind component, while over the subtropical western Atlantic both the evaporation and zonal wind are negatively correlated with the NAO index (Figs 2b and 2d).

c *The NAO and the Atlantic Thermohaline Circulation*

The positive NAO trend during 1970–99 communicates with the Atlantic Ocean climatic variables through precipitation, evaporation, wind forcing and atmospheric heating and

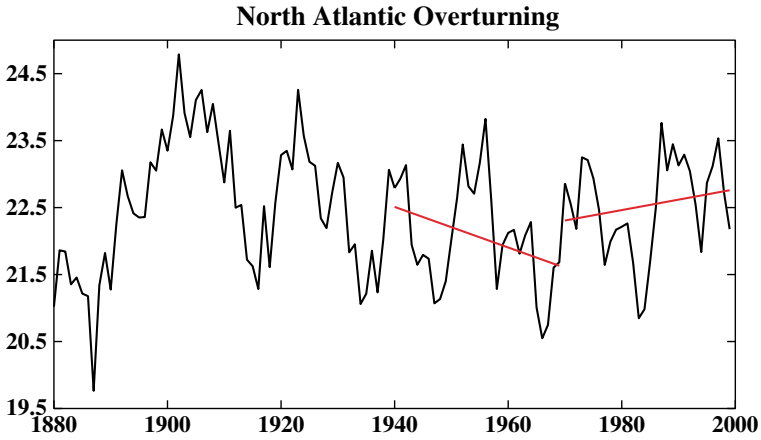

Fig. 3 Time series of the unsmoothed simulated annual ensemble-mean maximum of meridional overturning in the North Atlantic. Units are Sverdrups (10^6 m^3 s^{-1}). Linear trends for 1940–69 and 1970–99 are indicated by red lines.

cooling processes leading to changes in near-surface density in the subpolar regions of the North Atlantic. Observational analyses have documented that the surface air temperature warming is a response to increasing greenhouse gases. It is believed that the positive NAO trend during 1970–99 is not primarily forced by greenhouse gases. One possible confirmation for this might be the fact that during six of the last nine years, the Arctic Oscillation (AO) (the NAO is the local manifestation of the hemisphere-like AO phenomena, confined to the troposphere) has been either neutral or negative while at the same time an unprecedented temperature increase over the globe and over high latitude regions has been reported (Overland and Wang, 2005).

In our model with natural and anthropogenic forcings included, the global-mean surface air temperature increased by 0.53°C from 1880 to 1999, and a warming of 0.3°C occurred during the last three decades of the twentieth century. This overall warming is also reflected in a general increase in SST of 0.5°–1°C in the North Atlantic. In our transient warming simulations, the North Atlantic THC remains stable with a small decrease during 1940–69 and a slight increase during 1970–99 (Fig. 3). Since many climate models indicate a weakening of the THC in the North Atlantic in response to increased freshening and warming in this region (Manabe and Stouffer, 1999; Rahmstorf and Ganopolski, 1999; Russell and Rind, 1999; Wood et al., 1999; Hu et al., 2004), it would be of particular interest to look at the simulated interactions between the atmosphere and ocean and at the processes responsible for the stabilization of the THC in our model.

1 NAO AND OCEAN TEMPERATURE VARIABILITY

The well-known tripole structure for the interannual variability of surface ocean temperature in the North Atlantic (Wallace et al., 1990; Zorita et al., 1992; Grötzner et al., 1998) is reproduced in our experiment using both natural and anthropogenic forcing and presented as a correlation map between SST and the NAO index for the period 1970–99 (Fig. 4). From Fig. 4 it is seen that SST is negatively correlated with the NAO index in the area south-east of Greenland and in Baffin Bay and the Labrador Sea, as well as in the subtropics between 10°N and 25°N. Between these two centres of negative correlation, the simulated SST in the region of the subtropical gyre is positively correlated with the NAO index. The centre of this area is located in the western North Atlantic between 25°N and 45°N. The negative correlation between the surface temperature and the NAO index in the northern areas of the Atlantic and the Labrador Sea shows that the surface fluxes during the positive NAO tend to support cooling in the sinking regions of the North Atlantic.

The tripole pattern of SST and NAO index correlation is exhibited most clearly in our model when SST lags the NAO index by one year, and when SST is taken as an annual mean instead of the winter season average (Fig. 4). This lag reflects the ocean "memory" since the ocean accumulates the atmospheric forcing over time as the integration of local atmosphere-ocean heat and freshwater flux interactions. This lagged correlation between the NAO index and SST also suggests that the North Atlantic SST variability is not simply a response to low-frequency variations in the NAO. The advective-diffusive processes in the ocean influence the upper ocean temperature and salinity through propagation of thermal and saline anomalies from the subtropics to the subpolar regions in the North Atlantic. The advection of temperature and salinity anomalies from the tropics can either exaggerate or diminish the NAO influence on surface temperature and salinity in the North Atlantic, which will be shown later.

The ocean delay of the NAO index by one to two years was also noticed in the analysis of observational data for the intensity of the North Atlantic gyre circulation (Curry and McCartney, 2001) and it was shown that the ocean integrates both local and remote atmospheric NAO forcing over time along Lagrangian pathways.

Figure 5 shows the time series of unsmoothed simulated annual ensemble-mean SST, net heat flux at the atmosphere-ocean interface, and north-south heat transport of the upper 12 m ocean layer averaged over the area between 46°N and 58°N and 40°W and 55°W. (This area is marked on the correlation map, Fig. 4.) We chose this area for qualitative analysis of both temperature and salinity variability for 1970–99 because the largest convection and mixed layer depth changes occurred in this area of the North Atlantic in our model. As was mentioned before, the North Atlantic SST warmed by

0.5°–1°C over the last three decades. The SST over the area between 46°N and 58°N and 40°W and 55°W increased by 0.9°C from 1970 to 1999 (Fig. 5a).

Due to enhanced westerly winds over the North Atlantic between 45°N and 65°N for the period 1970–99 (Fig. 2b), evaporation greatly increased during the years with a strong Icelandic low phase (Fig. 2d), which caused ocean cooling from the enhanced latent heat flux as well as from the enhanced sensible heat flux from the ocean due to overall ocean warming. (Latent and sensible fluxes are considered to be negative in our model for heat loss from the ocean to the atmosphere.) Both the latent and sensible heat fluxes are negatively correlated with the NAO index over the Labrador Sea and over the area south of Greenland (not shown), which removes heat from the ocean.

Over the area between 46°N and 58°N and 40°W and 55°W, the net heat flux at the atmosphere-ocean interface (Fig. 5b) is negative indicating heat loss from the ocean. Although both evaporative and direct thermal ocean cooling increase during the period of the positive NAO trend, this is not enough to cause the decrease in SST in the North Atlantic. During the positive phase of the NAO, an increased northward heat transport (Fig. 5c) from the subtropical Atlantic plays the major role in the generation of a positive SST trend in the northern North Atlantic. It contributes about 98% to the first ocean layer temperature balance estimated over the area between 46°N and 58°N and 40°W and 55°W. Our model shows an enhancement of the Gulf Stream transport by 5% during 1970–99. The enhanced horizontal Gulf Stream transports act to compensate for the local SST cooling through surface heat fluxes that account for about 2% in the first ocean layer temperature balance.

The interannual, decadal and longer SST variability was first studied by Bjerknes (1964). He suggested that year-to-year SST fluctuations arise from heat fluxes at the atmosphere-ocean interface; on longer timescales, the changes in the ocean circulation play a primary role in SST variability. The conclusions of Bjerknes (1964) were confirmed by many later studies (Cayan, 1992a, 1992b; Deser and Blackmon, 1993; Kushnir, 1994; Halliwell, 1998; Walter and Graf, 2002; Wu and Gordon, 2002).

2 THE NAO AND OCEAN SALINITY VARIABILITY

Although both precipitation and evaporation are positively correlated with the NAO index (Figs 2c and 2d) and they increased in the area south of Greenland and over the Labrador Sea, the total freshwater flux has decreased over the same area, as well as over the sub-tropical Atlantic Ocean. During the positive phase of the NAO index, anomalously strong westerlies centred near 55°N and anomalous easterlies at about 35°N (Fig. 2b) tend to increase evaporation from the ocean surface (Fig. 2d), thereby contributing to the increase in salinity of the upper ocean. In the area of strong ocean convection, as well as in the tropical and subtropical Atlantic Ocean, the evaporation overwhelms the precipitation, resulting in an amplification of the positive surface salinity anomaly. As a result of this, unlike the surface ocean temperature, the sea surface salinity is positively correlated with the NAO index in the northern North Atlantic, as well as in the subtropical and tropical Atlantic Ocean (not shown).

Figure 6 shows the time series of unsmoothed simulated annual ensemble-mean sea surface salinity (SSS), total freshwater flux from the atmosphere to the ocean, and north-south salt transport in the upper 12 m ocean layer averaged over the area between 46°N and 58°N and 40°W and 55°W (this area is marked on the correlation map, Fig. 4). Surface salinity in this area increased by 0.17 psu from 1970 to 1999 (Fig. 6a). The reduced freshwater supply from the atmosphere to the ocean (Fig. 6b) favours the generation of a positive salinity anomaly in the area of maximum ocean mixing.

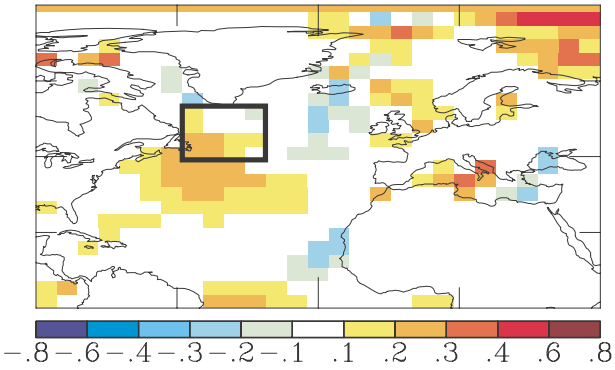

Fig. 4 Correlation map between the simulated ensemble-mean DJFM NAO index and the simulated annual ensemble-mean sea surface temperature for the period 1970–99. The SST lags the NAO index by one year.

The enhanced evaporation over the western tropical Atlantic resulted in a reduced freshwater flux and increased salinities in the area of the Gulf Stream, which is the major transport mechanism from the tropics to the high latitudes in the Atlantic Ocean. The enhanced horizontal Gulf Stream transport acts as an essential poleward transport of the salt anomaly (Fig. 6c) from the subtropics and contributes to increasing surface salinity in the North Atlantic area of enhanced winter convection.

Although both anomalous atmospheric freshwater flux and increased ocean advection of more saline waters into the area between 46°N and 58°N and 40°W and 55°W act in the same direction, increasing the SSS anomaly, the horizontal transports of salt from the subtropics play the major role in the salinity change, contributing about 97% to the surface salinity budget in this area. The reduced freshwater flux is of minor importance in our model adding only 3% to the SSS budget. Since the salinity is increasing in the area south of Greenland, the freshening effect of melting ice is overwhelmed by the increase in salinity due to increased salt transport from the south and the reduced freshwater flux at the ocean surface. So, the melting of sea ice due to overall warming plays a rather passive role in the area of active deep water formation, and its effect on the meridional overturning circulation is of lesser importance for the period 1970–99.

The observed small decrease in freshwater inflow over the Norwegian and Greenland seas and over the North Atlantic subpolar basins during 1996–2001 is reported by Peterson et al. (2006) and is based on an analysis of cumulative freshwater input anomalies from net precipitation, river discharge, net attrition of glaciers, and the Arctic Ocean sea-ice melt and export. The relatively small net freshwater decrease is explained by the fact that the subtropical saline inflows have slightly exceeded the Arctic freshwater outflows since 1995.

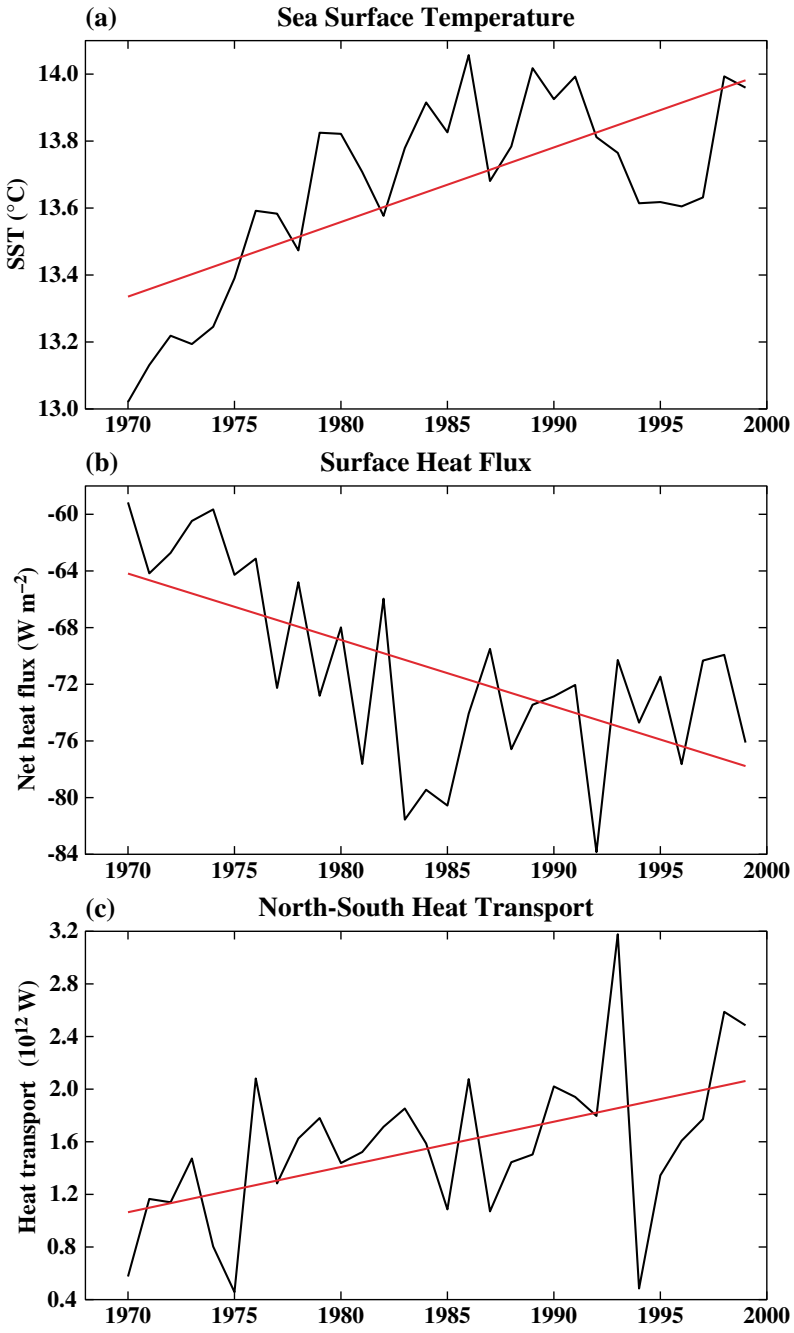

Fig. 5 Time series of unsmoothed simulated annual ensemble-mean SST, net heat flux at the atmosphere-ocean interface, and north-south heat transport of the upper 12-m ocean layer. All quantities are averaged over the area between 46°N and 58°N and 40°W and 55°W. Units for SST are °C; for net heat flux are W m^{-2}; for north-south heat transport are 10^{12} W. Linear trends for 1970–99 are indicated by red lines.

3 OCEAN CONVECTION AND THERMOHALINE CIRCULATION VARIABILITY

The density in the deep water formation regions is the key factor affecting the fluctuations in the intensity of the meridional overturning circulation. Density anomalies are partly associated with salinity and partly associated with temperature anomalies. In the area south of Greenland and the Labrador Sea, the positive upper ocean density anomaly (Fig. 7a) is mainly determined by anomalously salty conditions while contributions from increasing ocean temperatures are opposite in sign. The surface salinity increase overrides the counteracting enhanced warming in the high latitudes of the North Atlantic and plays a major role in the increase in surface density in the Labrador Sea and the ocean area south of Greenland, so that surface density is salinity driven in our model. The fact that the density anomaly and salinity anomaly are in phase and that density is determined by salinity is reflected in the strong correlation coefficient of 0.86 between density and salinity anomalies over the ocean area south of Greenland.

The increased surface density caused strengthening of the winter convection and deepening of the mixed layer depth in

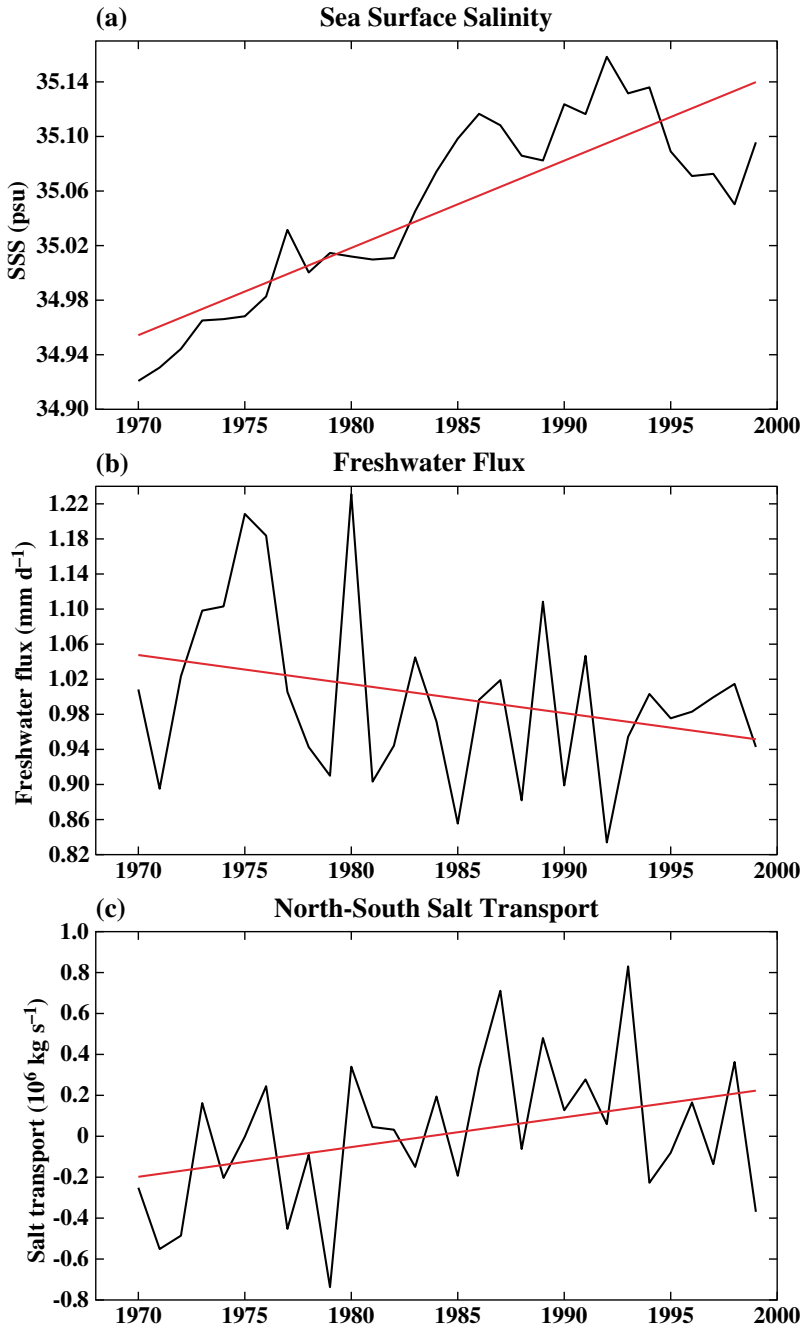

Fig. 6 Time series of unsmoothed simulated annual ensemble-mean SSS, freshwater flux, and north-south salt transport of the upper 12-m ocean layer. All quantities are averaged over the area between 46°N and 58°N and 40°W and 55°W. Units for SSS are practical salinity units (psu); for freshwater flux are mm d^{-1}; for north-south salt transport are 10^6 kg s^{-1}. Linear trends for 1970–99 are indicated by red lines.

the Labrador Sea and in the western North Atlantic (Fig. 7b). In the winter months, the modelled mixed layer depth is of order 1000 m in the North Atlantic, with the mixed layer depth being about 1500 m in a few places. In the Labrador Sea, the mixed layer depth becomes 100–150 m deeper during the winters of 1970–99, and the large area in the western North Atlantic becomes deeper by 50–75 m.

Our model results are consistent with observational data in the North Atlantic (Dickson et al., 1996) showing that the changing phase of the NAO is strongly connected with changes in convective activity in the northern areas of the Atlantic Ocean. In particular, the Labrador Sea convection is intense during the positive NAO phase, and it becomes increasingly suppressed in response to weakening westerly winds and the withdrawal of winter storm activity in the North Atlantic during low NAO index values.

The density change in the convection region leads the alteration of the meridional overturning circulation by several years suggesting that the upper ocean density anomalies precondition the stability of the ocean column and contribute to

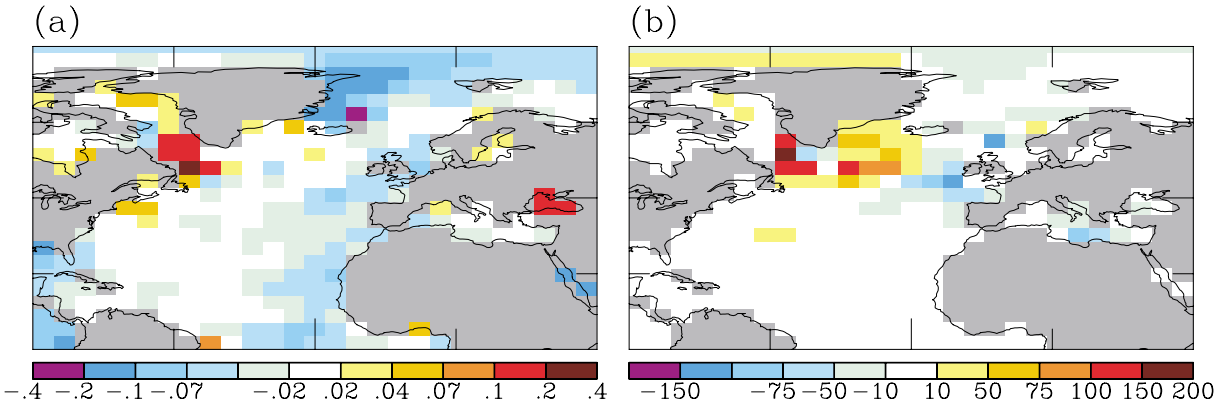

Fig. 7 Change based on the linear trend of simulated ensemble-mean DJFM (a) surface ocean density (kg m^{-3}); and (b) ocean mixed layer depth (m) for the period 1970–99.

the change in the intensity of the convection. Our model shows that the maximum correlation between the upper ocean density in the strong-mixing region and the meridional overturning circulation is equal to 0.56, and it is reached when the upper ocean density leads the meridional overturning circulation by four years.

The enhanced convection brings warmer water masses from lower layers to the surface, providing further heat loss from the ocean surface. This mechanism acts to damp the warm SST anomalies in the sinking area of the North Atlantic. The destabilization of the water column in the sinking area and the strength of the meridional overturning circulation in the North Atlantic are explained mainly by salinity anomalies over a large area of the western North Atlantic and the Labrador Sea, since the ocean densities in the cold subpolar regions are mainly determined by salinity.

The eastern part of the North Atlantic experiences an increased freshwater flux that, in conjunction with surface ocean warming, enhances the stability of the ocean column and leads to shallower convection in the winter (Fig. 7b). The contribution of reduced convection in the eastern North Atlantic to the overturning circulation is small, so it does not affect the increased meridional overturning circulation during the period 1970–99 (Fig. 3).

During the period of the positive trend of the NAO index, increased evaporation due to strong westerlies and increased horizontal transports of salt due to the strengthening of the Gulf Stream were the major contributors in creating the positive upper ocean density anomalies. This leads directly to an instability of the ocean column and causes an enhancement of deep water formation in areas south of Greenland. This in turn causes an intensification of the meridional overturning circulation. In our transient simulation with natural and anthropogenic forcing, the North Atlantic THC shows an increase in its intensity of approximately 2.5% during the positive phase of the NAO index.

The regression of surface heat flux versus the time series of the THC (not shown) exhibits a dominant pattern of heat flux variations associated with THC variability in our model which is quite similar to the pattern of heat flux anomalies associated with the NAO. The area south of Greenland, where the strong westerlies dominate during the positive NAO phase, and the subtropical area with strong easterlies are regions in the North Atlantic with heat loss. The regions offshore of the United States and in the north-eastern North Atlantic near Great Britain and Scandinavia are areas with positive surface heat flux anomalies. This heat flux regression versus THC from our model is consistent with modelling results from Delworth and Greatbatch (2000) and with the analysis of observational data by Cayan (1992a, 1992b).

4 Summary

Results of climate modelling with natural and anthropogenic forcings show that the intensity of the North Atlantic meridional circulation is closely connected with the atmospheric NAO. It is now believed that the positive trend of the NAO during the period 1970–99 is a manifestation of the internal variability of the coupled ocean-atmosphere system because the observational SLP data indicate either neutral or negative values for the NAO index starting in the late 1990s to the present (Cohen and Barlow, 2005). However, it is hypothesized that greenhouse gas forcing may be a contributing factor to the recent strengthening of the polar vortex and enhanced warming over high northern latitudes (Hurrell, 1996; Thompson et al., 2000).

Many climate models produce weakening of the North Atlantic THC in response to anthropogenic greenhouse warming (Manabe and Stouffer, 1999; Rahmstorf and Ganopolski, 1999; Russell and Rind, 1999; Wood et al., 1999; Hu et al., 2004), though the reduction is uncertain and model-variable in magnitude (Rahmstorf, 1999; Gregory et al., 2005; Schmittner et al., 2005).

Despite the global warming of 0.3°C and an overall increase in surface ocean temperature of 0.5°–1°C for the period 1970–99, our model experiments with both natural and anthropogenic forcings shows a stable THC in the North Atlantic. The meridional overturning circulation exhibits some strengthening during these three decades, which is in phase with the positive trend of the NAO index during this period. The positive trend of the NAO index resulted from a strengthened meridional pressure gradient due to decreased pressure over high polar latitudes and increased pressure over middle latitudes. Model experiments for the period 1970–99 reproduce SLP patterns consistent with observational data of

Arctic SLP (Walsh et al., 1996; Thompson and Wallace, 1998). Simulated regional surface air temperature and precipitation patterns are in agreement with large-scale patterns typical for the positive NAO trend (Hurrell, 1995; Thompson and Wallace, 2001).

Previously reported analyses of the North Atlantic SST (Cayan, 1992a, 1992b; Deser and Blackmon, 1993; Kushnir, 1994; Dickson et al., 1996; Grötzner et al., 1998; Delworth and Greatbatch, 2000; Curry and McCartney, 2001; Walter and Graf, 2002; Brauch and Gerdes, 2005) have shown that on interannual timescales the ocean surface over the North Atlantic is strongly influenced by the NAO, especially in the winter. In fact, the ocean surface temperature and salinity anomalies develop as a time-integrated response to persistent NAO air-sea heat and freshwater flux anomalies. However, on interdecadal timescales the ocean circulation may play a role in changing the thermohaline ocean structure (Deser and Blackmon, 1993; Kushnir, 1994).

The simulated tripole pattern of correlation between the SST and the NAO index is an oceanic response to atmospheric forcing associated with the NAO; it exhibits high heat loss in the subpolar North Atlantic and a large heat gain in the subtropical western North Atlantic during the positive phase of the NAO. The enhanced cold and dry westerly winds reproduced during the period of the positive NAO trend tend to extract more heat through anomalously large fluxes of sensible and latent heat. However, cooling of the upper ocean due to stronger westerly winds is overcompensated by the increased northward heat transport due to the enhanced Gulf Stream that contributes to the generation of the positive temperature anomalies. These warmed temperatures of the upper ocean layers act to increase the stability of the water column and suppress convection in the North Atlantic.

During the positive NAO trend, the increased evaporation due to strong westerly winds overwhelms the increased precipitation due to enhanced atmospheric moisture transport to the high latitudes under warming conditions, which leads to a reduced freshwater flux in the western part of the North Atlantic and as a result to the positive salinity anomalies of the upper ocean layer. The evaporation and salinity anomalies in the model's main sinking region south of Greenland vary in phase, so that during the upward NAO trend the atmosphere acts to amplify the positive salinity anomaly.

In addition to local subpolar NAO-coordinated influences of air-sea buoyancy fluxes to the upper ocean density, horizontal transport of salinity plays an important role in changing the stability of the ocean column. Our model reproduces anomalously high salinities in the western tropical Atlantic due to reduced freshwater fluxes under warming conditions. Strengthened northward currents south of Greenland promote further salinity import to the northern and north-western Atlantic. In fact, in our transient experiment with natural and anthropogenic forcing, the high salinity anomaly transport from the tropics to high latitudes plays the major role in increased salinity of the upper ocean layer in the North Atlantic, and reduced atmospheric freshwater flux further favours the generation of positive salinity anomalies.

Since the density increased in the area south of Greenland, we conclude that salinity dominates the evolution of density anomalies in the sinking regions in our simulation. Earlier modelling studies on the interdecadal variations of the THC in the North Atlantic (Delworth et al., 1993; Timmermann et al., 1998) demonstrated that near-surface density anomalies are strongly influenced by salinity anomalies north of approximately 55°N.

The salinity anomalies accumulate in the region south of Greenland until the density anomalies indicate that vertical stratification of the ocean column has become unstable which favours the initiation of deep convection. With a lag of four years, the meridional overturning circulation responds to the upper ocean density instability and enhanced convection and shows a strengthening of its cell in the North Atlantic. The increased northward transports of heat and salt through the enhanced Gulf Stream is part of the strengthened meridional circulation cell of the North Atlantic. The enhanced overturning circulation and increased horizontal transports are strongly supported by the reduced atmospheric freshwater fluxes during the positive NAO phase.

Our transient experiments with natural and anthropogenic forcing show that the ocean response to anomalous atmospheric conditions associated with the positive NAO trend over the last three decades of the twentieth century is a delay in THC weakening. However, a decreasing trend in the NAO index in the future could cause the acceleration of greenhouse gas induced weakening of the THC. Greenhouse-gas warming experiments with artificially induced trends of the AO-related surface fluxes (Delworth and Dixon, 2000) confirm this interpretation. In the experiments conducted by Delworth and Dixon (2000), the THC holds steady for about a decade and then declines in the twenty-first century experiments with an annual 1% greenhouse gas increase. The THC weakening is delayed by about 30–40 years since the THC strengthened during the period of the positive AO trend from years 1966 to 1995. Investigation of the behaviour of our model THC in the twenty-first century experiments will be done in the future and will be reported separately.

Acknowledgements

For this research, we acknowledge support from the NASA Earth Science Research Division. We thank Gary Russel, David Rind, Reto Ruedy and Gavin Schmidt for assistance in analysis of the experiments, Lilly Del Valle for technical assistance with the plots, and the reviewers for helpful comments.

References

BJERKNES, J. 1964. Atlantic air-sea interaction. *Adv. Geophys.* **10**: 1–82.

BRAUCH, J.P. and R. GERDES. 2005. Response of the northern North Atlantic and Arctic oceans to a sudden change of the North Atlantic Oscillation. *J. Geophys. Res*. **110**: C11018, doi:10.1029/2004JC002436.

CAYAN, D.R. 1992a. Latent and sensible heat flux anomalies over the Northern Oceans: The connection to monthly atmospheric circulation. *J. Clim.* **5**: 354–369.

CAYAN, D.R. 1992b. Latent and sensible heat flux anomalies over the Northern Oceans: Driving the sea surface temperature. *J. Phys. Ocean.* **22**: 859–881.

COHEN, J. and M. BARLOW. 2005. The NAO, the AO, and global warming: How closely related? *J. Clim.* **18**: 4498–4513.

CURRY, R.G. and M.S. MCCARTNEY. 2001. Ocean gyre circulation changes associated with the North Atlantic Oscillation. *J. Phys. Ocean.* **31**: 3374–3400.

DELWORTH, T.L.; S. MANABE and R.J. STOUFFER. 1993. Interdecadal variations of the thermohaline circulation in a coupled ocean-atmosphere model. *J. Clim.* **6**: 1993–2011.

DELWORTH, T.L. and L. GREATBATCH. 2000. Multidecadal thermohaline circulation variability driven by atmospheric surface flux forcing. *J. Clim.* **13**: 1481–1495.

DELWORTH, T.L. and K.W. DIXON. 2000. Implications of the recent trend in the Arctic/North Atlantic Oscillation for the North Atlantic thermohaline circulation. *J. Clim.* **13**: 3721–3727.

DESER, C. and M.L. BLACKMON. 1993. Surface climate variations over the North Atlantic Ocean during winter: 1900-1989. *J. Clim.* **6**: 1743–1753.

DICKSON, R.R.; J. LAZIER, J. MEINCKE, P. RHINES and J. SWIFT. 1996. Long-term coordinated changes in the convective activity of the North Atlantic, *Prog. Oceanogr.* **38**: 214–295.

FYFE, J.C.; G.J. BOER and G.M. FLATO. 1999. The Arctic and Antarctic Oscillations and their projected changes under global warming. *Geophys. Res. Lett.* **26**: 1601–1604.

GENT, P.R. 2001. Will the North Atlantic Ocean thermohaline circulation weaken during the 21st century? *Geophys. Res. Lett.* **28**: 1023–1026.

GENT, P.R. and J.C. McWilliams. 1990. Isopycnal mixing in ocean circulation models. *J. Phys. Ocean.* **20**: 150–155.

GREGORY, J.M.; K.W. DIXON, R.J. STOUFFER, A.J. WEAVER, E. DRIESSCHAERT, M. EBY, T. FICHEFET, H. HASUMI, A. HU, J.H. JUNGCLAUS, I.V. KAMENKOVICH, A. LEVERMANN, M. MONTOYA, S. MURAKAMI, S. NAWRATH, A. OKA, A.P. SOKOLOV and R.P. THORPE. 2005. A model intercomparison of changes in the Atlantic thermohaline circulation in response to increasing atmospheric CO_2 concentration. *Geophys. Res. Lett.* **32**: L12703, doi:10.1029/2005GL023209.

GRÖTZNER, A.; M. LATIF and T.P. BARNETT. 1998. A decadal climate cycle in the North Atlantic Ocean as simulated by the ECHO coupled GCM. *J. Clim.* **11**: 831–847.

HALLIWELL, G.R. JR. 1998. Simulation of North Atlantic decadal/multidecadal winter anomalies driven by basin-scale atmospheric circulation anomalies. *J. Clim.* **11**: 5–21.

HANSEN, J.; A. LACIS, D. RIND, G. RUSSEL, P. STONE, I. FUNG, R. RUEDY and J. LERNER. 1984. Climate sensitivity: Analysis of feedback mechanisms. In: *Climate Processes and Climate Sensitivity*, Geophys. Monogr. Ser., vol. 29, J.E. Hansen and T. Takahashi (Eds) , AGU, Washington, D.C. pp. 130–163.

HANSEN, J.; A. LACIS, R. RUEDY, M. SATO and H. WILSON. 1993. How sensitive is the world's climate? *Natl. Geogr. Res. Explor.* **9**: 142–158.

HANSEN, J.; M. SATO, L. NAZARENKO, R. RUEDY, A. LACIS, D. KOCH, I. TEGEN, T. HALL, D. SHINDELL, B. SANTER, P. STONE, T. NOVAKOV, L. THOMASON, R WANG, D. JACOB, S. HALLANDSWORTH, L. BISHOP, J. LOGAN, A. THOMPSON, R. STOLARSKI, J. LEAN, R. WILLSON, S. LEVITUS, J. ANTONOV, N. RAYNER, D. PARKER and J. CHRISTY. 2002. Climate forcings in Goddard Institute for Space Studies SI2000 simulations. *J. Geophys. Res.* **107**: 4347, doi:10.1029/2001JD001143.

HANSEN, J.; M. SATO, R. RUEDY, L. NAZARENKO, A. LACIS, G.A. SCHMIDT, G. RUSSELL, I. ALEINOV, M. BAUER, S. BAUER, N. BELL, B. CAIRNS, V. CANUTO, M. CHANDLER, Y. CHENG, A. DEL GENIO, G. FALUVEGI, E. FLEMING, A. FRIEND, T. HALL, C. JACKMAN, M. KELLEY, N. KIANG, D. KOCK, J. LEAN, J. LERNER, K. LO, S. MENON, R. MILLER, P. MINNIS, T. NOVAKOV, V. OINAS, JA. PERLWITZ, JU. PERLWITZ, D. RIND, A. ROMANOU, D. SHINDELL, P. STONE, S. SUN, N. TAUSNEV, D. THRESHER, B. WIELICKI, T. WONG, M. YAO and S. ZHANG. 2005. Efficacy of climate forcings. *J. Geophys. Res*. **110**: D18104, doi:10.1029/2005JD005776.

HU, A.; G.A. MEEHL, W.M. WASHINGTON and A. DAI. 2004. Response of the Atlantic thermohaline circulation to increased atmospheric CO_2 in a coupled model. *J. Clim.* **17**: 4267–4279.

HU, Z.-Z. and Z. WU. 2004. The intensification and shift of the annual North Atlantic Oscillation in a global warming scenario simulation. *Tellus*, **56A**: 112–124.

HURRELL, J.W. 1995. Decadal trends in the North Atlantic Oscillation: Regional temperatures and precipitation. *Science,* **169**: 676–679.

HURRELL, J.W. 1996. Influence of variations in extratropical wintertime teleconnections on Northern Hemisphere temperature. *Geophys. Res. Lett.* **23**: 665–668.

HURRELL, J.W. and H. VAN LOON. 1997. Decadal variations in climate associated with the North Atlantic Oscillation. *Clim. Change,* **36**: 301–326.

JONES, P.D.; T. JONSSON and D. WHEELER. 1997. Extension to the North Atlantic Oscillation using early instrumental pressure observations from Gibraltar and south-west Iceland. *Int. J. Climatol.* **17**: 1433–1450.

KUSHNIR, Y. 1994. Interdacadal variations in North Atlantic sea surface temperature and associated atmospheric conditions. *J. Clim.* **7**: 141–157.

LARGE, W.G.; J.C. MCWILLIAMS and S.C. DONEY. 1994. Oceanic vertical mixing: a review and a model with a nonlocal boundary layer parameterization. *Rev. Geophys.* **32**: 363–403.

LATIF, M.; E. ROECKNER, U. MIKOLAJEWICZ and R. VOSS. 2000. Tropical stabilization of thermohaline circulation in a greenhouse warming simulation. *J. Clim.* **13**: 1809–1813.

MANABE, S. and R.J. STOUFFER. 1999. The role of thermohaline circulation in climate. *Tellus,* **51A-B**: 91–109.

OSBORN, T.J. 2004. Simulating the winter North Atlantic Oscillation: The roles of internal variability and greenhouse gas forcing. *Clim. Dyn.* **22**: 605–623.

OSBORN, T.J.; K.R. BRIFFA, S.F.B. TETT, P.D. JONES and R.M. TRIGO. 1999. Evaluation of the North Atlantic Oscillation as simulated by a coupled climate model. *Clim. Dyn.* **15**: 685–702.

OSTERMEIER, G.M. and J.M. WALLACE. 2003. Trends in the North Atlantic Oscillation-Northern Hemisphere Annular Mode during the twentieth century. *J. Clim.* **16**: 336–341.

OVERLAND, J.E. and M. WANG. 2005. The Arctic climate paradox: The recent decrease of the Arctic Oscillation. *Geophys. Res. Lett.* **32**: L06701, doi: 10.1029/2004GL021752.

PETERSON, B.J.; J. MCCLELLAND, R. CURRY, R.M. HILMES, J.E. WALSH and K. AAGAARD. 2006. Trajectory shifts in the Arctic and subarctic freshwater cycle. *Science*, **313**: 1061–1066.

RAHMSTORF, S. 1999. Shifting seas in the greenhouse? *Nature*, **399**: 523–524.

RAHMSTORF, S. and A. GANOPOLSKI. 1999. Long-term global warming scenarios computed with an efficient coupled model. *Clim. Change,* **43**: 353–367.

ROGERS, J. and H. VAN LOON. 1979. The seesaw in winter temperatures between Greenland and northern Europe: Part 2. Some oceanic and atmospheric effects in middle and high latitudes. *Mon. Weather Rev.* **107**: 509–519.

RUSSELL, G.L. and D. RIND. 1999. Response to CO_2 transient increase in the GISS coupled model: Regional cooling in a warming climate. *J. Clim.* **12**: 531–539.

SCHMIDT, G.A.; R. RUEDY, J.E. HANSEN, I. ALEINOV, N. BELL, M. BAUER, S. BAUER, B. CAIRNS, V. CANUTO, Y. CHENG, A. DEL GENIO, G. FALUVEGI, A.D. FRIEND, T.M. HALL, Y. HU, M. KELLEY, N.Y. KIANG, D. KOCH, A.A. LACIS, J. LERNER, K.K. LO, R.L. MILLER, L. NAZARENKO, V. OINAS, JA. PERLWITZ, D. RIND, A. ROMANOU, G.L. RUSSELL, M. SATO, D.T. SHINDELL, P.H. STONE, S. SUN, N. TAUSNEV, D. THRESHER and M.-S. YAO. 2006. Present day atmospheric simulations using GISS ModelE: Comparison to in-situ, satellite and reanalysis data. *J. Clim*. **19**: 153–192.

SCHMITTNER, A.; M. LATIF and B. SCHNEIDER. 2005. Model projections of the North Atlantic thermohaline circulation for the 21st century assessed by observations. *Geophys. Res. Lett.* **32**: L23710, doi:10.1029/2005GL024368.

SHINDELL, D.T.; R.L. MILLER, G.A. SCHMIDT and L. PANDOFLO. 1999. Simulation of recent northern winter climate trends by greenhouse-gas forcing. *Nature*, **399**: 452–455.

SUN, S. and R. BLECK. 2001. Atlantic thermohaline circulation and its response to increasing CO_2 in a coupled atmosphere-ocean model. *Geophys. Res. Lett.* **28**: 4223–4226.

THOMPSON, D.W.J. and J.M. WALLACE. 1998. The Arctic Oscillation signature in the wintertime geopotential height and temperature fields. *Geophys. Res. Lett.* **25**: 1297–1300.

THOMPSON, D.W.J.; J.M. WALLACE and G.C. HEGERL. 2000. Annular modes in the extratropical circulation. Part II. Trends. *J. Clim.* **13**: 1018–1036.

THOMPSON, D.W.J. and J.M. WALLACE. 2001. Regional climate impacts of the Northern Hemisphere Annular Mode. *Science*, **293**: 85–89.

TIMMERMANN, A.; M. LATIF, R. VOSS and A. GROTZNER. 1998. Northern hemispheric interdecadal variability: a coupled air-sea mode. *J. Clim.* **11**: 1906–1931.

VAN LOON, H. and J. ROGERS. 1978. The seesaw in winter temperatures between Greenland and northern Europe: Part 1. General description. *Mon. Weather Rev*. **106**: 296–310.

VISBECK, M.; H. CULLEN, G. KRAHMANN and N. NAIK. 1998. An ocean model's response to North Atlantic Oscillation-like wind forcing. *Geophys. Res. Lett.* **25**: 4521–4524.

WALLACE, J.M.; C. SMITH and Q. JIANG. 1990. Spatial patterns of atmospheric-ocean interaction in the northern winter. *J. Clim.* **3**: 990–998.

WALSH, J.E.; W.L. CHAPMAN and T.L. SHY. 1996. Recent decrease of sea level pressure in the central Arctic. *J. Clim.* **9**: 480–486.

WALTER, K. and H.-F. GRAF. 2002. On the changing nature of the regional connection between the North Atlantic Oscillation and sea surface temperature. *J. Geophys. Res.* **107**: 4338, doi:10.1029/2001JD000850.

WOOD, R.A.; A.B. KEEN, J.F.B. MITCHELL and J.M. GREGORY. 1999. Changing spatial structure of the thermohaline circulation in response to atmospheric CO_2 forcing in a climate model. *Nature,* **399**: 572–575.

WU, P. and C. GORDON. 2002. Oceanic influence on North Atlantic climate variability. *J. Clim.* **15**: 1911–1925.

ZORITA, E.; V. KHARIN and H. VON STORCH. 1992. The atmospheric circulation and sea-surface temperature in the North Atlantic area in winter: Their interaction and relevance for Iberian precipitation. *J. Clim.* **5**: 1097–1108.